JACS
JOURNAL OF THE AMERICAN CHEMICAL SOCIETY
Article
pubs.acs.org/JACS

Ultrafast Infrared Spectroscopy on Channelrhodopsin-2 Reveals Efficient Energy Transfer from the Retinal Chromophore to the Protein

Mirka-Kristin Neumann-Verhoefen,[†] Karsten Neumann,[†] Christian Bamann,[‡] Ionela Radu,[§] Joachim Heberle,[⊥] Ernst Bamberg,[‡] and Josef Wachtveitl*,[†]

[†]Institute of Physical and Theoretical Chemistry, Johann Wolfgang Goethe-University Frankfurt, Max-von-Laue Strasse 7, 60438 Frankfurt am Main, Germany

[‡]Max Planck Institute of Biophysics, Max-von-Laue Strasse 3, 60438 Frankfurt am Main, Germany

[§]Department of Physics, Molecular Biospectroscopy, Freie Universität Berlin, Arnimallee 14, 14195 Berlin, Germany

[⊥]Department of Physics, Experimental Molecular Biophysics, Freie Universität Berlin, Arnimallee 14, 14195 Berlin, Germany

ABSTRACT: The primary reaction dynamics of channelrhodopsin-2 was investigated using femtosecond vis-pump/mid-IR probe spectroscopy. Due to the fast deactivation of the excited state in channelrhodopsin-2, it is possible to observe the direct impact of retinal isomerization on the protein surrounding. We show that the dominant negative band at 1665 cm^{-1} tentatively assigned to an amide I vibration is developed with a time constant of 0.5 ps. Also a variety of side-chain vibrations are formed or intensified on this time scale. The comparison of the light-induced FT-IR spectra of channelrhodopsin-2 in H_2O and D_2O at 80 K enabled us to tentatively identify the contribution of Arg side chain(s). The subsequently observed decay of nearly the whole difference pattern has a particularly high impact on the C═C and C═N stretching vibrations of the retinal. This suggests that the underlying mechanism describes a cooling process in which the excess energy is redirected toward the retinal surrounding, e.g., the protein and functional water molecules. The pronounced protein contributions in comparison to other rhodopsins point to a very efficient energy redistribution in channelrhodopsin-2.

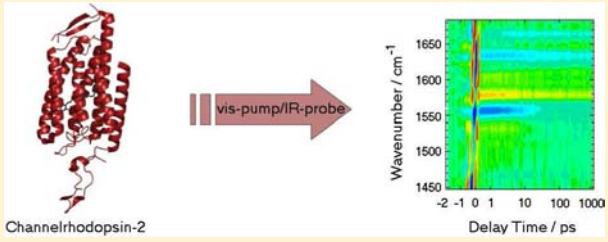

INTRODUCTION

The green alga *Chlamydomonas reinhardtii* possesses seven opsin-like genes (termed COP), which encode retinal-containing proteins.[1] Among those, the ion channels channelrhodopsin-1 (ChR1) and channelrhodopsin-2 (ChR2) are responsible for the phototactic and photophobic response of the algae.[2,3] For ChR1, it was first assumed that the channel is only permeable for protons.[4] More recent results obtained at higher pH values show that both ChR1 and ChR2 are also permeable for Na^+, Li^+, and Ca^{2+}.[5,6] In recent years, especially ChR2 became particularly known for its application in neurobiology because it depolarizes cells within milliseconds after blue-light excitation. Together with the archaeal halorhodopsin (HR) which hyperpolarizes cells after yellow-light stimulus, ChR2 is most successfully used in the field of optogenetic control.[7−10]

The present study focuses on the photochemical characterization of ChR2's seven transmembrane motif (amino acids 1−315).[6] The residual approximately 400 amino acids belong to a cytoplasmic domain with an up to now unknown function.[11] Both the projection structure and the resulting homology model of ChR2[11] as well as the high resolution X-ray structure of a ChR1/ChR2 chimera[12] show that ChR2 exhibits a high structure consistency with the archaeal retinal protein bacteriorhodopsin (BR). For helix C in which, for example, the homologue of BR's proton acceptor (ChR2: Glu123; BR: Asp85) is found, ChR2 and BR exhibit a very high sequence homology.[6] Unlike other rhodopsins, both ChR structures argue for a dimer as functional unit of ChR.[11,12] Asp253 (homologous to BR Asp212) rather than Glu123 is supposed to be the major proton acceptor as inferred from electrophysiological experiments on protein variants where these residues have been exchanged.[12] Glu83 or Glu90 are proposed as the potential proton donor.[12−16] His134, the homologue of Asp96 in BR, is hydrogen bonded to Glu83.[12]

The high relevance of ChRs initiated a series of spectroscopic and electrophysiological studies over recent years.[1,13,15,17−25] Resonance Raman and retinal extraction experiments thereby showed that approximately 70% of the retinal chromophores are in the all-*trans* and the residual fraction in the 13-*cis* configuration. After light adaptation, the isomer composition does not change significantly. Only an additional small population (5%) of presumably 9-*cis*-retinal is observable.[20] Our vis-pump/vis-probe measurements showed that the deactivation of the excited state, e.g. the retinal isomerization and K photoproduct formation, takes place on identical time scales as in BR and in sensory rhodopsin II (SRII).[23,26] After a fast vibrational relaxation of the excited state population with 150 fs its decay with mainly 400 fs was observed. Thus, both the initial

Received: January 17, 2013
Published: March 28, 2013

 © 2013 American Chemical Society dx.doi.org/10.1021/ja400554y | *J. Am. Chem. Soc.* 2013, 135, 6968−6976

all-*trans*-retinal ground state and the 13-*cis*-retinal K photoproduct are populated. The reaction proceeds in the electronic ground state with a 2.7 ps component assigned to a vibrational cooling process. It is therefore likely that the isomerization mechanism for ChR2 is similar to that proposed for BR.[27,28] Also, flash photolysis experiments revealed the appearance of the first red-shifted ground-state intermediate, K-like (P_1^{500}), within nanoseconds.[15,19] As the transition to the subsequent intermediate is thermally activated, the early P_1^{500} state can be trapped at low temperature. The light-induced FT-IR spectrum of ChR2 at 80 K revealed that the retinal underwent the all-*trans* to 13-*cis* isomerization in this state.[15,22] The observation of a strong negative band in the amide I region was surprising because it has not been observed for retinal proteins to this extent previously.[15,22] Radu et al. interpreted this amide I change as an indication for pore formation[22] that prepares the protein to open the ion gate at a later stage. The subsequent M-like (P_2^{390}state) intermediate is formed with a time constant of 4 μs. Due to its absorption maximum at 390 nm, one can assume that the Schiff base exists in its deprotonated form, like in BR.[27,28] Studies on ChR mutants suggest that the channel shows first ion permeability already at this stage.[17] The main conductive state is the subsequent red-shifted photocycle intermediate P_3^{520}. Recently, it was shown that the rise and decay of this intermediate concur with proton release and uptake.[24] Proton pumping by ChR2 was demonstrated in the absence of a membrane potential.[29] Nack et al. refer to a mechanistic link between the channel ion conducting and the proton pumping mode.[24] The closing of the channel is observed with time constants in the range of 10−30 ms.[18,29] From a spectroscopic point of view, a spectrally silent transition to a further red-shifted photoproduct takes place. The channel is desensitized including the repopulation of the initial all-*trans*-retinal ground state with a very large time constant of 5 s.[15,22] The temperature independence of this component demonstrates that the photocycle is most likely completed through a series of individual steps.[26] FT-IR measurements point to the fact that the hydrogen bonding network of the ground state is restored in this process.[22]

In the present paper, we continue our ultrafast studies of ChR2[23,26] using the structure-sensitive method of fs-vis-pump/IR-probe spectroscopy. Additional insights in the chromophore protein coupling are gained. Of particular interest is thereby the formation dynamics of the difference band in the amide I region, which was assigned to a conformational protein change.[22]

MATERIALS AND METHODS

Light-Induced FT-IR Difference Spectroscopy. Light-induced FT-IR difference spectra at 80 K were recorded with a spectral resolution of 4 cm^{-1} as previously described.[22] Briefly, 5 μL of a highly concentrated solution of ChR2 (pH and pD of 7.4) was added to a sandwich cell of two BaF_2 substrates which were inserted into a LN_2 cryostat (Oxford Instruments Limited, Abingdon, UK). Sample excitation was performed by a light-emitting diode (Luxeon Star, Brantford, Canada, emission maximum at 462 and 30 nm FWHM, power density of 10 mW/cm^{-2}). FT-IR difference spectra were calculated by subtraction of the dark state spectrum from the intermediate state spectrum of the sample recorded under continuous illumination at 80 K.

Vis-Pump/IR-Probe Spectroscopy. The transient absorption measurements were performed using a ChR2 sample (truncated construct, amino acids 1−315) solubilized in *n*-decyl-β-D-maltopyranoside (DM). A description of the protein extraction and the purification can be found elsewhere.[17] Due to the high absorption of water in the mid-IR spectral region, the measurements were performed on ChR2 in buffered D_2O solution (20 mM 4-(2-hydroxyethyl)-1-piperazineethanesulfonic acid (HEPES), pD 7.4, 0.2% DM, 100 mM NaCl). To obtain a significant H/D exchange, the sample was stored in the D_2O buffer for two weeks. The sample was concentrated to a final optical density of about 0.15 at 450 nm in a CaF_2 cuvette with a 50 μm path length using centrifugal filters (Centriprep, 50 kD cutoff, Millipore, Schwalbach, Germany).

The ultrafast pump/probe experiment is based on a Clark CPA 2001 laser (Clark-MXR, Dexter, MI), which provides pulses at a central wavelength of 775 nm, a pulse duration of 170 fs, and a repetition rate of 1 kHz. A general description of the experimental setup is given by Neumann et al.[30] Excitation pulses with a central wavelength of 430 nm (absorption spectrum of ChR2 depicted in Figure 1a) and a pulse energy of 400 nJ were generated by sum frequency mixing[32] of noncollinear optical parametric amplifier (NOPA)[33,34] pulses and laser fundamental pulses.

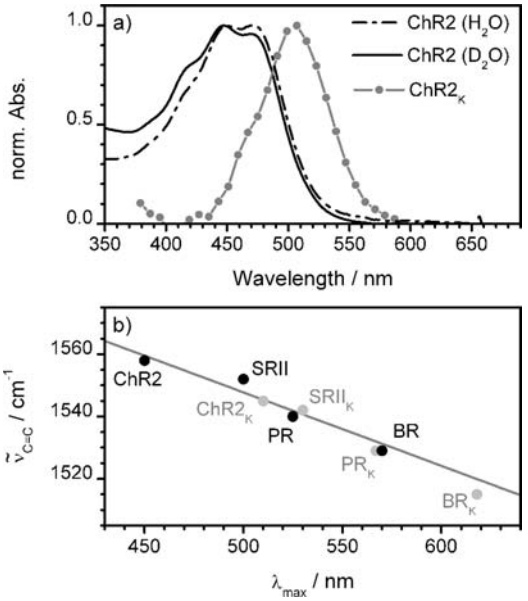

Figure 1. (a) Normalized UV−vis absorption spectra of ChR2 in D_2O (black solid line) and H_2O (dashed-dotted line) and the calculated spectrum of the $ChR2_K$ state (gray line with dots); the H_2O data set is taken from ref 26. (b) Linear dependence of the visible absorption maximum and the frequency of the C=C stretching vibration of some selected retinal proteins in the ground and the K state (data taken from refs 26, 30, and 31).

The probe pulses were created using a two-stage optical parametric amplifier (OPA) and subsequent difference frequency generation (DFG) of the OPA signal and idler pulses. For the probed spectral region, three measurements were performed in the range between 1450 cm^{-1} to 1520 cm^{-1}, 1520 cm^{-1} to 1585 cm^{-1}, and 1585 cm^{-1} to 1680 cm^{-1}, in each case with two overlapping channels. Pump and probe pulses were polarized in the magic angle with respect to each other, resulting in isotropic transient absorption signals. The cross-correlation widths of the experiments were 300 fs to 350 fs depending on the wavenumber. The exchange of the sample between two successive laser shots was provided by simultaneous rotation and translation of the sample.

To our knowledge, the UV/vis absorption spectra of pure all-*trans*- or 13-*cis*-retinal ChR2 samples are unknown to date. Therefore, we cannot strictly exclude that besides the predominant all-*trans* configuration of the retinal also the *cis* isomer is excited in our experiments. Wand et al. showed that the initial retinal configuration influences the internal conversion and photoisomerization dynamics of BR.[35] However, for ChR2 at least the variation of the excitation wavelength from 420 to 480 nm does not cause dynamic changes of the electronic transitions.[26]

For the quantitative data analysis, we used a kinetic model that describes the data as the sum of exponential decays. A Marquart

dx.doi.org/10.1021/ja400554y | J. Am. Chem. Soc. 2013, 135, 6968−6976

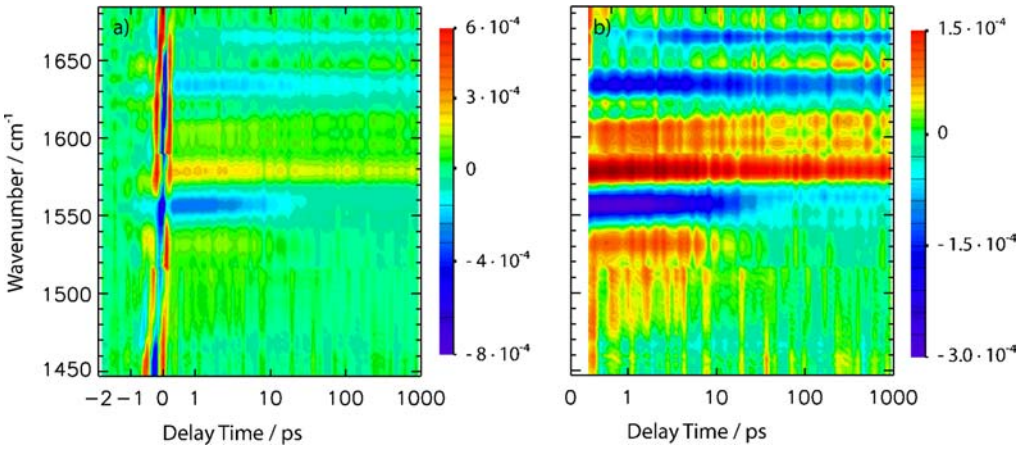

Figure 2. Two-dimensional representation of the transient absorbance changes of ChR2 in the region of 1450 cm^{-1} to 1690 cm^{-1} after excitation at 430 nm. The *x*-axis is linearly scaled up to 1 ps and logarithmic afterward. The absorbance changes are color coded: red = positive, green = zero, and blue = negative signals. The color is adjusted to the highest positive and negative signal. Because the cross-phase modulation around time zero has a significantly higher amplitude ($-8 \times 10^{-4} \leq \Delta A \leq 6 \times 10^{-4}$) compared to the sample signal ($-3 \times 10^{-4} \leq \Delta A \leq 1.5 \times 10^{-4}$) we added a rescaled second plot (b), in which only the photoinduced signals of the sample are shown.

downhill algorithm optimizes n global time constants τ_i for all wavelengths simultaneously with wavelength dependent amplitudes $A_i(\lambda)$ for each component. Our model function assumes Gaussian pump and probe pulses with a $(1/e)$ cross-correlation width t_{cc}:

$$\Delta A(t, \lambda) = \sum_{i=1}^{n} A_i(\lambda) \exp\left(\frac{t_{cc}^2}{4\tau_i^2} - \frac{t}{\tau_i}\right)\frac{1}{2}\left(1 + \mathrm{erf}\left(\frac{t}{t_{cc}} - \frac{t_{cc}}{2\tau_i}\right)\right)$$

The n wavelength-dependent fit amplitudes $A_i(\lambda)$ represent the decay-associated spectra (DAS) for each component. In this definition, an infinite time constant is equal to a time-independent offset ($t \gg t_{cc}$) in the transient absorbance changes, and hence it mainly corresponds to the residual signal at the maximum delay time in our experiments (1.8 ns). In our case, strong coherent signatures due to the perturbed free induction decay (PFID)[36,37] and the cross-phase modulation[38,39] are observed at negative delay times and around time zero. These effects cannot be corrected by subtracting the corresponding spectra of the solvent, e.g., the buffer. We therefore restricted the data analysis to delay times >0.3 ps.

RESULTS

Steady-State Visible Absorption Spectroscopy. Figure 1a shows the ground state absorption spectra of ChR2 at pH 7.4 and pD 7.4 with their characteristic vibrational fine structure. The spectrum taken in D_2O well resembles the one recorded in H_2O. The main electrostatic properties around the chromophore should thus be the same under both conditions.

Femtosecond Time-Resolved IR Spectroscopy. Figure 2a provides an overview about the photoinduced transient absorbance changes of ChR2 in the spectral region between 1450 cm^{-1} and 1690 cm^{-1}. The absorbance changes are color coded (for more detailed information, see the caption of Figure 2). Effects at negative delay times can be traced back to PFID,[36,37] whereas the signal around time zero is dominated by the cross-phase modulation.[38,39] The unperturbed photoinduced dynamics of the sample are monitored at delay times >0.3 ps. A plot illustrating only these contributions is depicted in Figure 2b. It shows a multitude of positive and negative difference bands. In a first step, the single contributions are therefore presented with decreasing wavenumber of the band position (Figure 3).

Around 1665 cm^{-1}, a clear negative difference signature is visible. The band is formed on a subpicosecond time scale and possesses a constant amplitude of -0.1×10^{-3} at delay times >2 ps (Figure 3a). Blue and red-shifted to this band are two small positive signatures. Another strong negative difference band is evident at 1635 cm^{-1}. Because it exhibits the PFID at negative delay times, the band is attributed to a chromophore ground-state vibration. At short delay times, a positive contribution is

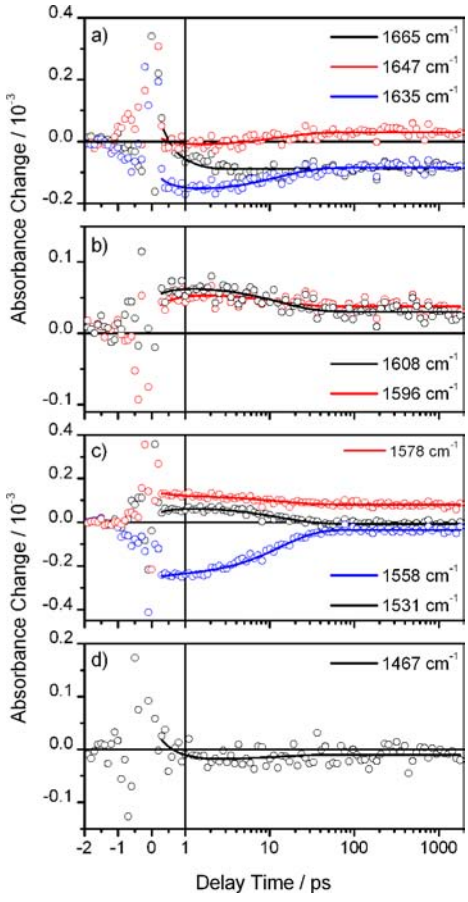

Figure 3. Transient absorbance changes of ChR2 at selected wavenumbers after excitation at 430 nm. The raw data are displayed as dots and the global fit as a solid line. The *y*-axis is scaled for an optimal visualization of the photoinduced reaction. As a consequence, part of the cross-phase modulation around time zero had to be cut off.

dx.doi.org/10.1021/ja400554y | J. Am. Chem. Soc. 2013, 135, 6968−6976

visible around 1600 cm^{-1}. It splits into two features with increasing delay times which slightly shift to the red or the blue, respectively (Figures 3b and 4a). It is likely that a superimposed

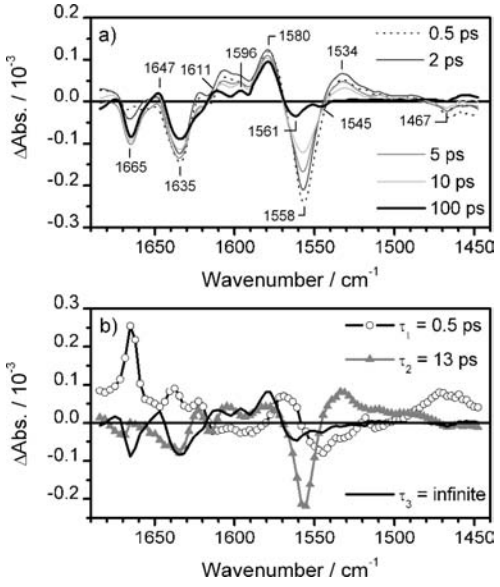

Figure 4. (a) Transient spectra (raw data) of ChR2 at selected delay times colored in gray scale. (b) Decay-associated spectra of the global fit analysis of the photoinduced data. A fit using three decay components leads to a satisfactory description of the data.

negative band is the origin of this feature. The most intense positive band of the examined spectral region is found around 1580 cm^{-1}. A positive absorbance change of 0.15×10^{-3} is monitored directly after the cross-phase modulation (Figure 3c). The further time course shows only a small decay component on a 10 ps time scale. Around 1558 cm^{-1}, a strong and broad negative difference band is visible. This contribution decays and gets narrower on a 10 ps time scale. At long delay times (t_D > 100 ps), two negative difference bands centered at 1545 cm^{-1} and 1561 cm^{-1} are observed. The PFID at 1555 cm^{-1} indicates that at least one of these bands is a chromophore ground-state vibration. A positive absorbance change is monitored red-shifted to the negative bands (Figure 4a). It decays with the same temporal behavior (Figure 3c). Next to this band a broad (1520 cm^{-1} to 1470 cm^{-1}) positive contribution is visible. It has very small amplitude and decays with a 10 ps time constant. On the low-frequency edge of the investigated spectral region, a small negative band is apparent at 1467 cm^{-1}. It is formed on a subpicosecond time scale and stays constant afterward (Figure 3d).

Band Assignment. Because the spectroscopic investigations of ChR2 started only a few years ago, few vibrational bands have been assigned. What makes things more difficult is the fact that the early IR difference spectra of BR and ChR2 strongly differ so that reasoning by analogy is only valid to a minor degree. Nevertheless, possible assignments are presented in the following section. However, they cannot be regarded as complete; further studies are indispensable.

The signature of the PFID around 1555 cm^{-1} allows the assignment of the strong negative signature in this spectral region to a ground-state vibration of the retinal chromophore. The pronounced characteristics of this band in resonance Raman experiments[20] strongly suggest an attribution to the C=C stretching vibration of the retinal. This assumption is further supported by the linear dependence of the visible absorption maximum of the retinal and the frequency of the C=C stretching vibration.[40,41] Figure 1b shows that the visible absorption maximum of ChR2 at 450 nm should result in a C=C bleaching band around 1560 cm^{-1}, as observed here. Absorption maxima of the side bands λ_{max} = 420 and 470 nm yield C=C bleaching bands at $\tilde{\nu}_{CC}$ = 1566 cm^{-1} and 1555 cm^{-1}, respectively. In analogy to other retinal proteins (Figure 1b), the $ChR2_K$ product vibration should be found at lower wavenumbers. We calculated the visible absorption maximum of the K state by subtracting the ground-state spectrum from the $ChR2_K$ − ChR2 difference spectrum recorded at 1.5 ns (Figure 1a, data set taken from ref 26). The $ChR2_K$ absorption maximum was found at approximately 510 nm which should cause a C=C stretching vibration at 1548 cm^{-1}. A relatively broad positive signature is observed in this spectral region at short delay times but not visible at the end of the observation time, however (Figures 4a, 5b). A positive C=C stretching band red-shifted to

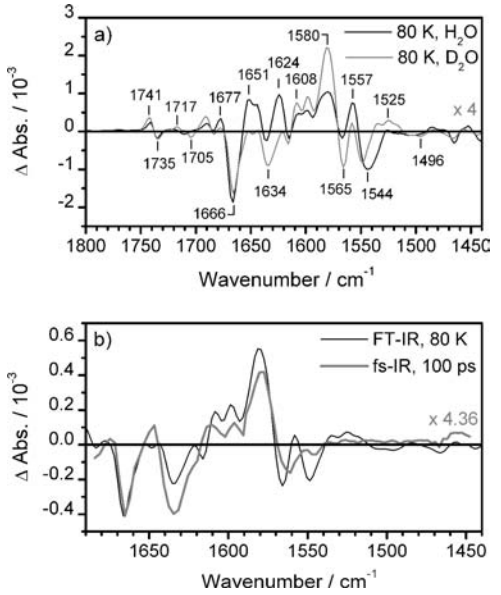

Figure 5. (a) Comparison of the light-induced difference spectra of ChR2 in H_2O (black trace) and D_2O (gray trace) recorded at 80 K. The spectra were scaled to the same intensity at 1735 cm^{-1}. (b) Comparison of the 80 K difference spectrum (black trace) with the transient spectrum at 100 ps (gray trace). Both spectra were recorded in D_2O and have been scaled to the same intensity at 1665 cm^{-1}.

the ground-state bleaching band has also not been observed in the respective $ChR2_K$ − ChR2 difference spectrum recorded at 80 K in H_2O (Figure 5a).[22] However, the low temperature light-induced difference spectrum taken in D_2O buffer shows a small but broad positive contribution centered at 1525 cm^{-1}. In contrast, our transient spectrum at 100 ps reveals a small negative signature at 1545 cm^{-1} (Figures 4a, 5b). This may be interpreted in the way that the positive signal of the $ChR2_K$ C=C stretching vibration is superimposed by a negative band. Also, the respective light-induced difference spectrum at 80 K shows a negative signature at this spectral position, although it has higher amplitude (Figure 5a). To our knowledge, the origin of the negative band is unknown to date. An attribution to a (local) amide II mode could explain the effect in a H_2O sample. Because our measurements were performed in D_2O, a putative amide II band should be drastically reduced in intensity because only

dx.doi.org/10.1021/ja400554y | J. Am. Chem. Soc. 2013, 135, 6968−6976

marginal parts of the protein have not been exchanged (Figure 5a). Therefore, it seems improbable that changes in the amide II band would fully compensate for the positive C=C stretching band of $ChR2_K$.

The most intense positive band is observed at 1580 cm^{-1}. Directly after excitation, the band exhibits high amplitude and only slightly decays on a 10 ps time scale (Figure 3c). Also, for this band, the assignment to an amide II mode is unlikely for the above-mentioned reasons. The signal height also excludes the possibility that it is due to the spectral shift of a vibration of a single amino acid. However, the crystal structure of a ChR chimera shows a multitude of polar amino acids (Glu, Asp, Tyr, Arg) in the immediate vicinity of the retinal.[12] The side chains of all these amino acids have distinct vibrational bands around 1570 cm^{-1} to 1590 cm^{-1}.[42]

The difference bands in the subsequent spectral region up to 1615 cm^{-1} are dominated by two bands which change their band position with increasing delay times. This behavior can be explained by a superimposed negative species. On the basis of the present literature, none of the three bands can be assigned. The small amplitudes suggest that they originate from a perturbation or a change of a single amino acid side chain. According to Barth,[42] Arg, Tyr, or His side chains may contribute to the observed difference signal.

The negative band around 1635 cm^{-1} can be certainly assigned to a retinal ground-state vibration due to the distinct signature of the PFID. Also, in this case the resonance Raman experiments are very helpful. For ChR2 in H_2O, Nack et al.[20] showed a band appearing at 1657 cm^{-1}, which is assigned to the C=N stretching vibration of the Schiff base. Upon deuteration, this band shifts to 1629 cm^{-1}, indicating the strong coupling of the C=N and the N−H or N−D vibrations. The negative band at 1635 cm^{-1} observed in this study is therefore assigned to the C=N stretching vibration of the chromophore system. This assignment is corroborated by the fact that the time evolution of the transient at this wavenumber resembles that of the C=C stretching band around 1560 cm^{-1} (Figure 3a and 3c). The small positive band around 1647 cm^{-1} may be a result of the difference signal of a Gln or Asn residue. In contrast to the negative band at 1635 cm^{-1}, the assignment of the strong negative signal at 1665 cm^{-1} is not as clear. At negative delay times, only a very weak negative signal is observed. The origin of this feature could again be the PFID of another chromophore ground-state vibration (e.g., the C=N stretching vibration of undeuterated sample[20]) or more likely it must be traced back to the oscillatory signature of the PFID of the C=N vibration of the retinal Schiff base at 1635 cm^{-1}. The putatively high H/D exchange rate of the Schiff base proton argues against the assignment to the C=N stretching vibration of the protonated Schiff base. Also the temporal behavior of the transient at 1665 cm^{-1} clearly differs from those of the C=N (1635 cm^{-1}) and C=C (1560 cm^{-1}) stretching vibrations (Figure 3a and 3c). While the latter exhibits the maximal amplitude at $t_D = 0$, the band at 1665 cm^{-1} is formed on a subpicosecond time scale. Also the subsequent dynamics bears significant differences: The two retinal ground-state bands (1635 cm^{-1} and 1560 cm^{-1}) exhibit strong changes on a 10 ps time scale, whereas the signature at 1665 cm^{-1} stays constant after 2 ps. An alternative assignment of the band at 1665 cm^{-1} is the attribution to a difference signal of one or more amino acid side chains. However, a single amino acid most likely does not cause such a large difference signal. Low temperature FT-IR experiments also showed the appearance of a strong negative band at this position[15,22] and assigned it to the amide I vibration. The fact that this difference band is formed on a 500 fs time scale points to a rearrangement of the C=O oscillators near the retinal binding pocket. If this assignment is correct, a corresponding amide II′ mode should be present. Unfortunately, the signal-to-noise ratio is slightly poorer in the respective spectral region between 1450 cm^{-1} and 1480 cm^{-1}. Nevertheless, the formation of a negative band at 1467 cm^{-1} is observable on a 500 fs time scale (Figure 3d). The very weak intensity of this difference band may be explained by the fact that the amide II′ vibration is not as sensitive to structural changes as the amide I vibration. The band at 1467 cm^{-1} could also be due to a bleach of a HDO vibration.

Global Fit Analysis. For a quantitative analysis, the data were modeled by a sum of exponentials. To avoid perturbing effects of the cross-phase modulation, the data were fitted for delay times ≥0.3 ps. The three subsequently recorded spectral regions were modeled both individually and collectively; the deviations of the time constants and the respective DAS are negligible. Although a variety of difference bands had to be modeled, the whole data set can be optimally described using three decay constants. The first two time constants have values of $\tau_1 = 0.5$ ps and $\tau_2 = 13$ ps. The last component was set to infinite and models the residual signal at very long delay times. The corresponding amplitude spectrum therefore resembles the transient spectrum after 1.8 ns (identical to depicted 100 ps spectrum). Table 1 summarizes the obtained time constants and contrasts them with the time constants determined by the global analysis of a pump/probe data set recorded in the visible spectral range.[23,26]

Table 1. Comparison of the Time Constants Obtained in Global Fit Analyses of the Vis Pump/Vis Probe[23,26] and Vis Pump/IR Probe Data Sets of ChR2

	τ/ps	τ/ps	τ/ps	τ
vis pump/vis probe	<0.1	0.4	2.7	∞
vis pump/IR probe	–	0.5	13	∞

Figure 4b shows the DAS of the time components obtained in the global fit procedure. The spectral characteristics of τ_1 can be explained as follows: The broad positive signature between 1450 cm^{-1} and 1500 cm^{-1} originates from the small rise of the negative signal in this spectral region. Around 1470 cm^{-1}, an insection is visible which can be traced back to the formation of the negative band (putatively assigned to an amide II′ vibration) at this position. The negative amplitude at 1534 cm^{-1} shows the generation of the vibrationally hot and therefore red-shifted C=C stretching band. Also, τ_1 has a significant influence on the negative bleaching characteristics of this vibration. The positive amplitude around 1570 cm^{-1} corresponds to the decrease of the blue shoulder of the bleach band. The DAS of τ_1 shows a structured negative characteristic in the adjacent region. It is ascribed to the formation of positive bands in this spectral range. In the region of the C=N stretching vibration, the positive amplitude at 1635 cm^{-1} is indicative for the further small decrease of this band. The most prominent feature of the DAS of τ_1 is found at 1665 cm^{-1}. This contribution describes the formation of the strong negative band in this region. Subsuming, it can be stated that the process connected to τ_1 consists of three main contributions: First, the negative signatures due to the C=C and the C=N stretching vibration of the retinal ground state become slightly more negative with this time constant. This might be attributed to the fact that superimposed positive bands (vibrationally hot and thus broad contributions) decay on this

dx.doi.org/10.1021/ja400554y | J. Am. Chem. Soc. 2013, 135, 6968−6976

time scale. Second, the formation of the dominant C=C product band (1534 cm^{-1}) is connected to τ_1. Third, a variety of further positive and negative bands are formed with this time constant, among others the prominent band at 1665 cm^{-1}. These signatures are most likely not connected to the chromophore but to the protein surrounding. All these processes can be explained by the decay of the first excited state, i.e., the isomerization of the chromophore, which was observed on this time scale in transient absorption experiments in the visible region.[23,26] The present IR data monitor well the direct impact of the retinal isomerization on the protein.

The DAS of τ_2 significantly differs from that of τ_1. Almost in the whole spectral region a slight decay of positive and negative difference bands is observed with this component. Especially the bleached ground-state bands of the C=C and C=N stretching vibrations ((−)1555 cm^{-1}, (−)1634 cm^{-1}) as well as the product signature of the C=C mode ((+)1534 cm^{-1}) of the retinal chromophore are affected. Thus, we infer that τ_2 is connected to a cooling process in which the vibrational energy is passed on to chromophore low frequency modes as well as to the surrounding water molecules and to the protein moiety. Interestingly, the DAS of τ_2 has no amplitude in the region of the putative amide I band at 1665 cm^{-1}, which means that this band is not affected by the decrease of the molecular temperature of the system. Yet, an explanation for this finding cannot be given.

Light-Induced FT-IR Difference Spectra at 80 K. The 80 K difference spectrum of deuterated ChR2 samples shows remarkable deviations from that recorded in H_2O (Figure 5a).

In the region specific to amide II vibrations of the protein backbone (~1550 cm^{-1}), the strong negative band at 1544 cm^{-1} becomes narrower and shifts to 1548 cm^{-1} in the D_2O spectrum, suggesting that the band contains contributions of amide II vibrations. The corresponding amide II′ mode is difficult to be identified in the D_2O spectrum, but the band at 1496 cm^{-1} might be a good candidate. The low intensity might be due to the presence of an overlapping positive band. Indeed, at higher frequencies, the band at (+)1557 cm^{-1} becomes weaker in the D_2O spectrum, pointing to contributions from amide II modes that are downshifted upon exposure to D_2O. The shift of the amide II band at 1544 cm^{-1} reveals the negative band at 1548 cm^{-1} and a broad positive spectral feature that peaks at 1525 cm^{-1}. The former is due to the C=C symmetric stretch mode of the all-*trans*-retinal in the ground state as shown by resonance Raman spectroscopy.[20] The exact assignment of the latter is difficult, but it may include contributions of the C=C symmetric stretch mode of the retinal in the red-shifted photoproduct. At higher frequencies, the negative band at 1565 cm^{-1} gains intensity in the D_2O spectrum. The C=C symmetric stretch mode of the 13-*cis* form of the retinal in the ground state is expected to contribute at this frequency consistent with Raman data.[20] In the region specific to amide I vibrations of the protein backbone (1620−1690 cm^{-1}), the strong negative band at 1666 cm^{-1} is present in both the H_2O and the D_2O spectrum. The fact that this band is not altered in the D_2O spectrum and also manifests in the transient spectra at 100 ps (Figure 5b) indicates, once again, that ChR2 undergoes conformational changes in the peptide bond as soon as on the subnanosecond time scale. The negative band at 1634 cm^{-1} observed in the D_2O spectrum contains contributions from the C=N stretching mode of the Schiff base as shown by Raman spectroscopy.[20]

Remarkably, the positive bands at 1624, 1651, and 1677 cm^{-1} vanish in the D_2O spectrum, indicating that they do not originate from amide I modes. The band at 1651 cm^{-1} may include the C=N−H stretch mode of the retinal Schiff base in this early intermediate. The frequency of the corresponding C=N−D stretch in D_2O is difficult to determine, but the positive bands at 1608 or 1599 cm^{-1} are prime candidates. The frequencies of the bands at 1624 and 1677 cm^{-1} are consistent with arginine stretching vibrations. Upon deuteration, these are down-shifted to 1608 and 1580 cm^{-1}, respectively.[43] Surprisingly, the corresponding negative bands cannot be found in the spectrum, which implies that they are shifted and compensated by the stronger positive bands. These observations may suggest that arginine side chains underwent alterations such as hydrogen bonding changes already in this early intermediate.

Under these circumstances, the positive amide I bands reflecting the change in protein secondary structure are not present in the D_2O spectra. Probably, they are less localized on a particular amide I mode (less ordered) and are compensated by the more ordered and more intense negative bands.

In the C=O region indicative of protonated carboxylic amino acid side chains, the difference band at (+)1741/(−)1735 cm^{-1} was attributed to hydrogen bonding changes of D156 upon the transition to the early intermediate.[22,25] The insensitivity toward H/D exchange is surprising but has been reported for the same band occurring during the lifetime of the P_4 state.[15] At lower wavenumbers, the weak bands at (+)1722/(−)1711 cm^{-1} are down-shifted to (+)1717/(−)1705 cm^{-1} in the D_2O spectrum together with a gain in intensity. In the absence of relevant site-directed mutants, it is not clear if such a complex spectral feature originates from changes of the protonation states and/or H-bonding interactions of several carboxylic residues.

Previous FT-IR studies on ChR2 at 80 K showed that the difference bands between 1740 and 1540 cm^{-1} originating from blue light-induced structural changes of both protein and retinal chromophore (see above) are reverted upon green light illumination (λ = 520 nm), as demonstrated by the mirror image difference spectra.[15] Such spectral behavior is consistent with a strong retinal−protein coupling in ChR2, as suggested in the present study.

DISCUSSION

The primary reaction dynamics of ChR2 was studied using vis-pump/IR-probe spectroscopy. The inherent sensitivity of vibrational spectroscopy thereby enabled us to monitor not only the photoinduced changes of the retinal chromophore but also the response of the apoprotein.

Tentative Band Assignment. In the investigated spectral region between 1680 cm^{-1} and 1450 cm^{-1}, a variety of positive and negative difference bands are observable after photoexcitation. The ground-state vibrations of the retinal chromophore can be unambiguously disentangled from the other bands by the unique signature of the PFID at negative delay times. According to this effect, the ground-state C=N stretching vibration of the retinal Schiff base link is found at 1635 cm^{-1} (D_2O) and the C=C stretching vibration at 1560 cm^{-1}. Both band positions agree with those found in resonance Raman measurements.[20] Due to the linear dependence of the visible absorption maximum and the position of the C=C stretching frequency,[40,41] the positive contribution of the $ChR2_K$ C=C stretching vibration is also assigned. Accordingly, we found a positive signature at 1534 cm^{-1} which exhibits a dynamics like the depleted ground-state retinal vibrations. At the maximum delay time of our experiment, this signature is absent; however, a small negative band remains. The $ChR2_K$ product vibration is therefore most likely superimposed by another band.

dx.doi.org/10.1021/ja400554y | J. Am. Chem. Soc. 2013, 135, 6968−6976

Table 2. Summary of the Most Important Vibrational Contributions and Their Preliminary Assignment

vibration/cm^{-1}	tentative assignment
(−)1665 cm^{-1}	localized amide I vibration
(−)1635 cm^{-1}	C═N−D stretch of the retinal Schiff base in ground-state ChR2
(+)1611 (fs-IR)/1608 cm^{-1} (80 K FT-IR) (+)1580 cm^{-1}	C═N stretching modes of deuterated Arg side chains
(−)1560 (fs-IR)/1565 cm^{-1} (80 K FT-IR)	C═C stretch ground state
(+)1534 cm^{-1}	C═C stretch product state

Besides these retinal vibrations, the remaining strong positive and negative difference signals are attributed to amino acid side chain or local protein backbone vibrations. The most striking band at 1665 cm^{-1} is assigned to a localized amide I change by the insensitivity to H/D-exchange (see Figure 5a). It cannot be excluded that the signal also contains a contribution of amino acid side-chain vibrations, e.g., the C═O vibration of an Asn or Gln. The formation dynamics of the band at 1665 cm^{-1} strongly hints to the fact that this local rearrangement of the peptide C═O vibrations is an immediate consequence of the retinal isomerization. The residual difference bands can be attributed to amino acid side-chain vibrations. The fact that the positive band at 1580 cm^{-1} is present directly after the decay of the cross-phase modulation indicates that this vibration is strongly perturbed by the excitation of the chromophore. The respective functional group(s) should therefore be located in the immediate vicinity of the chromophore. Likely candidates for the difference band are the asymmetric COO^- vibration of Asp/Glu, the C═C vibration of His, and/or C−N stretching vibrations of Arg. The observed positive difference bands at 1611 cm^{-1} and 1596 cm^{-1} (100 ps spectra, Figure 4a) seem to be rather sensitive to the molecular temperature of the system, because a small, but distinct, shift of the bands is observed on a 10 ps time scale. Besides the mentioned Arg vibrations, His ($HisH_2^+$ ν(C═C)) and Tyr (Tyr−O^- ν(CC) or Tyr-OH ν(CC)δ(CH)) vibrations might also contribute to these difference bands. A clear-cut assignment of all side-chain bands cannot be given at this stage. Studies using site-directed mutants are currently being performed. However, the comparison of the light-induced difference spectra of ChR2 in H_2O and D_2O buffer recorded at 80 K (Figure 5a) reveals that some particular side-chain modes are very sensitive to the structural changes induced by the isomerization of the retinal. The positive bands peaking at 1624 cm^{-1}, and 1677 cm^{-1} in the H_2O spectra disappear in D_2O. They probably shift to 1580 cm^{-1} and to 1608 cm^{-1} upon deuteration. Due to their band position in the infrared spectra, they are tentatively assigned to arginine residues. The recent report on the crystal structure of a ChR1−ChR2 chimera highlighted the relevance of Arg174 and Arg120 (Arg82 in BR) for ChR2 functionality.[12]

Efficient Energy Transfer from the Chromophore to the Protein. The analysis of the recorded time-resolved data set shows that some of the difference bands already exhibit a large signal amplitude after the cross-phase modulation and further rise with a time constant of τ_1 = 0.5 ps; other bands such as the tentatively assigned amide I and amide II′ vibrations at 1665 cm^{-1} and 1467 cm^{-1} are formed with this time constant. A comparison to transient absorption measurements performed in the visible spectral range as well as a fluorescence upconversion experiment reveals that the process associated with this time constant must be ascribed to the deactivation of the excited state, e.g., the isomerization of the chromophore. The formation of the amide bands with this time constant thereby directly proves that the isomerization of the retinal in ChR2 does not only cause distortions of the side chains and the H-bonding network in the vicinity of the retinal but also highly affects the local protein backbone. Thus, the ion channel ChR2 does not only exhibit a speed-optimized retinal isomerization dynamics but is also constructed to efficiently transfer the excess energy to the protein. Kato et al. concluded that a motion of the C-terminal end of TM1 opens the pore exit formed by TM1, TM2, and TM7. However, because no direct interaction between TM1 and the chromophore is observed in the crystal structure, the energy of retinal isomerization must be transferred to this helix via movements of TM2, TM3, and/or TM7. Our study strongly supports this suggestion, as a very strong chromophore protein coupling is monitored.

The time constant of τ_2 = 13 ps describes a decay of the whole difference pattern except for the band at 1665 cm^{-1}. The depleted ground-state vibrations of the C═C and C═N stretching vibration are particularly influenced. Thus, we concluded that the connected component describes a cooling process on the vibrationally hot ground-state potential (S_1 deactivation occurs within approximately 500 fs[26]). Thus, the excess energy of the all-*trans*- and 13-*cis*-retinal population is transferred to retinal low frequency modes as well as the chromophore surroundings, e.g., protein backbone, side chains, and functional water molecules. This leads to an overall decrease of the molecular temperature. Compared to the transient absorption experiments performed in the visible region,[23,26] a significantly larger time constant of 13 ps is observed for the cooling process following the excited-state deactivation in the corresponding IR experiment. This does not necessarily mean that a different transition is observed in this case. The process in the IR also contains contributions of energy distribution from the chromophore to the protein, internal vibrational redistribution of the chromophore into low frequency modes, and vibrational cooling in the surrounding protein. Usually, cooling is accompanied by strong shifts in the vibrational band position as well as changes in the bandwidth. Here we observe only for the retinal vibrations ($\nu(C{=}C)_{GS}$ = 1555 cm^{-1}, $\nu(C{=}C)_{K}$ = 1534 cm^{-1}, and $\nu(C{=}N)_{GS}$ = 1634 cm^{-1}) of ChR2 and for the side-chain modes peaking at 1596 and 1611 cm^{-1} (at 100 ps) alterations in the band position and the bandwidth. In contrast, the huge amide I band at 1665 cm^{-1} is completely unaffected by this process. Overall, the energy dissipation in ChR2 is very efficient.

Comparison to Other Retinylidene Proteins. The comparison of the observed photoinduced vibrational dynamics of ChR2 to the bacterial retinal protein proteorhodopsin (PR)[30] shows major differences. For PR, the long lifetime of the excited state leads to a variety of vibrationally hot populations during the first 20 ps, which are located in the excited state as well as in the all-*trans* and 13-*cis* ground states. This results in a superposition of broad, mostly red-shifted chromophore vibrations, which hampers the general band assignment. Also, the transfer of the excess energy to the proteins seems not to be as pronounced as in ChR2. Contributions of the apoprotein show up only as a small negative amide I band[30,44,45] or a positive amide II signature

dx.doi.org/10.1021/ja400554y | J. Am. Chem. Soc. 2013, 135, 6968−6976

which in this case was visualized by selective labeling.[30] Photoinduced side-chain vibrations were sparsely observed.[45] Although the excited-state deactivation processes of the archaeal proton pump BR, the phototaxis sensor SRII, and the cation channel ChR2 are very similar, the photoinduced vibrational spectra of BR and SRII exhibit much less pronounced difference bands ascribed to the protein backbone.[46−48] Side-chain vibrations are virtually not detected. Assuming that the extinction coefficients of the vibrational bands and the quantum yield of K formation are similar for ChR2 and the mentioned rhodopsin, the chromophore protein coupling, e.g., the energy transfer, must thus be clearly more efficient in ChR2. Also, for rhodopsin (Rh), an ultrafast isomerization (approximately 200 fs) and a strong coupling of the retinal chromophore to the protein are observed.[49−52] However, to the authors' knowledge, no ultrafast IR data are published yet, which rules out any comparison.

CONCLUSION

From our vis-pump/IR-probe measurements, it is evident that ChR2 retinal isomerization has a very high impact on the protein surrounding. Some side-chain difference bands already appear within excitation; the pronounced difference band at 1665 cm^{-1} most likely originating from an amide I vibration is formed with a time constant of 500 fs. The ultrafast formation of this contribution supports a very strong chromophore protein coupling. In comparison to BR, SRII, and PR, the early light-induced IR spectra of ChR2 exhibit considerably more side-chain difference bands and an enlarged amide I contribution. We therefore conclude that the energy transfer from the retinal to the opsin moiety does not correlate with the isomerization speed. The combined photophysical and structural conditions in ChR2 seem to be a case *sui generis* among retinal proteins. Thus, it is perfectly suited for a comprehensive study addressing the implications of retinal isomerization on the structural changes of the protein matrix. However, an extensive band assignment is indispensable for this concern.

AUTHOR INFORMATION

Corresponding Author

wveitl@theochem.uni-frankfurt.de

Notes

The authors declare no competing financial interest.

ACKNOWLEDGMENTS

This work was supported by grants from the Deutsche Forschungsgemeinschaft SFB-807 (J.W. and E.B.), Center of Excellence Frankfurt (J.W. and E.B.), and SFB-1078 and FOR-1279 (J.H.). I.R. acknowledges financial support from the Focus Area Nanoscale of the Freie Universität Berlin.

REFERENCES

(1) Stehfest, K.; Hegemann, P. *ChemPhysChem.* **2011**, *11*, 1120−1126.
(2) Foster, K. W.; Saranak, J.; Patel, N.; Zarilli, G.; Okabe, M.; Kline, T.; Nakanishi, K. *Nature* **1984**, *311*, 756−759.
(3) Sineshchekov, O. A.; Jung, K. H.; Spudich, J. L. *Proc. Natl. Acad. Sci. U.S.A.* **2002**, *99*, 8689−8694.
(4) Nagel, G.; Ollig, D.; Fuhrmann, M.; Kateriya, S.; Mustl, A. M.; Bamberg, E.; Hegemann, P. *Science* **2002**, *296*, 2395−2398.
(5) Berthold, P.; Tsunoda, S. P.; Ernst, O. P.; Mages, W.; Gradmann, D.; Hegemann, P. *Plant Cell* **2008**, *20*, 1665−1677.
(6) Nagel, G.; Szellas, T.; Huhn, W.; Kateriya, S.; Adeishvili, N.; Berthold, P.; Ollig, D.; Hegemann, P.; Bamberg, E. *Proc. Natl. Acad. Sci. U.S.A.* **2003**, *100*, 13940−13945.
(7) Boyden, E. S.; Zhang, F.; Bamberg, E.; Nagel, G.; Deisseroth, K. *Nat. Neurosci.* **2005**, *8*, 1263−1268.
(8) Zhang, F.; Prigge, M.; Beyriere, F.; Tsunoda, S. P.; Mattis, J.; Yizhar, O.; Hegemann, P.; Deisseroth, K. *Nat. Neurosci.* **2008**, *11*, 631−633.
(9) Zhang, F.; Wang, L. P.; Brauner, M.; Liewald, J. F.; Kay, K.; Watzke, N.; Wood, P. G.; Bamberg, E.; Nagel, G.; Gottschalk, A.; Deisseroth, K. *Nature* **2007**, *446*, 633−U4.
(10) Deisseroth, K. *Nat Meth.* **2011**, *8*, 26−29.
(11) Müller, M.; Bamann, C.; Bamberg, E.; Kühlbrandt, W. *J. Mol. Biol.* **2011**, *414*, 86−95.
(12) Kato, H. E.; Zhang, F.; Yizhar, O.; Ramakrishnan, C.; Nishizawa, T.; Hirata, K.; Ito, J.; Aita, Y.; Tsukazaki, T.; Hayashi, S.; Hegemann, P.; Maturana, A. D.; Ishitani, R.; Deisseroth, K.; Nureki, O. *Nature* **2012**, *482*, 369−374.
(13) Eisenhauer, K.; Kuhne, J.; Ritter, E.; Berndt, A.; Wolf, S.; Freier, E.; Bartl, F.; Hegemann, P.; Gerwert, K. *J. Biol. Chem.* **2012**, *287*, 6904−6911.
(14) Sugiyama, Y.; Wang, H.; Hikima, T.; Sato, M.; Kuroda, J.; Takahashi, T.; Ishizuka, T.; Yawo, H. *Photochem. Photobiol. Sci.* **2009**, *8*, 328−336.
(15) Ritter, E.; Stehfest, K.; Berndt, A.; Hegemann, P.; Bartl, F. J. *J. Biol. Chem.* **2008**, *283*, 35033−35041.
(16) Ruffert, K.; Himmel, B.; Lall, D.; Bamann, C.; Bamberg, E.; Betz, H.; Eulenburg, V. *Biochem. Biophys. Res. Commun.* **2011**, *410*, 737−743.
(17) Bamann, C.; Gueta, R.; Kleinlogel, S.; Nagel, G.; Bamberg, E. *Biochemistry* **2009**, *49*, 267−278.
(18) Bamann, C.; Kirsch, T.; Nagel, G.; Bamberg, E. *J. Mol. Biol.* **2008**, *375*, 686−694.
(19) Ernst, O. P.; Murcia, P. A. S.; Daldrop, P.; Tsunoda, S. P.; Kateriya, S.; Hegemann, P. *J. Biol. Chem.* **2008**, *283*, 1637−1643.
(20) Nack, M.; Radu, I.; Bamann, C.; Bamberg, E.; Heberle, J. *FEBS Lett.* **2009**, *583*, 3676−3680.
(21) Nikolic, K.; Grossman, N.; Grubb, M. S.; Burrone, J.; Toumazou, C.; Degenaar, P. *Photochem. Photobiol.* **2009**, *85*, 400−411.
(22) Radu, I.; Bamann, C.; Nack, M.; Nagel, G.; Bamberg, E.; Heberle, J. *J. Am. Chem. Soc.* **2009**, *131*, 7313−7319.
(23) Scholz, F.; Bamberg, E.; Bamann, C.; Wachtveitl, J. *Biophys. J.* **2012**, *102*, 2649−2657.
(24) Nack, M.; Radu, I.; Schultz, B.-J.; Resler, T.; Schlesinger, R.; Bondar, A.-N.; del Val, C.; Abbruzzetti, S.; Viappiani, C.; Bamann, C.; Bamberg, E.; Heberle, J. *FEBS Lett.* **2012**, *586*, 1344−1348.
(25) Nack, M.; Radu, I.; Gossing, M.; Bamann, C.; Bamberg, E.; von Mollard, G. F.; Heberle, J. *Photochem. Photobiol. Sci.* **2010**, *9*, 194−198.
(26) Verhoefen, M.-K.; Bamann, C.; Blöcher, R.; Förster, U.; Bamberg, E.; Wachtveitl, J. *ChemPhysChem.* **2010**, *11*, 3113−3122.
(27) Lanyi, J. K. *J. Phys. Chem. B* **2000**, *104*, 11441−11448.
(28) Oesterhelt, D. *Curr. Opin. Struct. Biol.* **1998**, *8*, 489−500.
(29) Feldbauer, K.; Zimmermann, D.; Pintschovius, V.; Spitz, J.; Bamann, C.; Bamberg, E. *Proc. Natl. Acad. Sci. U.S.A.* **2009**, *106*, 12317−12322.
(30) Neumann, K.; Verhoefen, M.-K.; Weber, I.; Glaubitz, C.; Wachtveitl, J. *Biophys. J.* **2008**, *94*, 4796−4807.
(31) Verhoefen, M.-K.; Lenz, M. O.; Amarie, S.; Klare, J. P.; Tittor, J.; Oesterhelt, D.; Engelhard, M.; Wachtveitl, J. *Biochemistry* **2009**, *48*, 9677−9683.
(32) Kozma, I. Z.; Baum, P.; Lochbrunner, S.; Riedle, E. *Opt. Express* **2003**, *11*, 3110−3115.
(33) Riedle, E.; Beutter, M.; Lochbrunner, S.; Piel, J.; Schenkl, S.; Sporlein, S.; Zinth, W. *Appl. Phys. B: Laser Opt.* **2000**, *71*, 457−465.
(34) Wilhelm, T.; Piel, J.; Riedle, E. *Opt. Lett.* **1997**, *22*, 1494−1496.
(35) Wand, A.; Friedman, N.; Sheves, M.; Ruhman, S. *J. Phys. Chem. B* **2012**, *116*, 10444−10452.
(36) Hamm, P. *Chem. Phys.* **1995**, *200*, 415−429.
(37) Wynne, K.; Hochstrasser, R. M. *Chem. Phys.* **1995**, *193*, 211−236.
(38) Ekvall, K.; van der Meulen, P.; Dhollande, C.; Berg, L. E.; Pommeret, S.; Naskrecki, R.; Mialocq, J. C. *J. Appl. Phys.* **2000**, *87*, 2340−2352.
(39) Lorenc, M.; Ziolek, M.; Naskrecki, R.; Karolczak, J.; Kubicki, J.; Maciejewski, A. *Appl. Phys. B: Lasers Opt.* **2002**, *74*, 19−27.

(40) Aton, B.; Callender, R. H.; Becher, B.; Ebrey, T. G. *Biochemistry* **1977**, *16*, 2995−2999.
(41) van den Berg, R.; Jang, D. J.; Bitting, H. C.; El-Sayed, M. A. *Biophys. J.* **1990**, *58*, 135−141.
(42) Barth, A. *Biochim. Biophys. Acta* **2007**, *1767*, 1073−1101.
(43) Braiman, M. S.; Briercheck, D. M.; Kriger, K. M. *J. Phys. Chem. B* **1999**, *103*, 4744−4750.
(44) Amsden, J. J.; Kralj, J. M.; Chieffo, L. R.; Wang, X. H.; Erramilli, S.; Spudich, E. N.; Spudich, J. L.; Ziegler, L. D.; Rothschild, K. J. *J. Phys. Chem. B* **2007**, *111*, 11824−11831.
(45) Rupenyan, A.; van Stokkum, I. H. M.; Arents, J. C.; van Grondelle, R.; Hellingwerf, K.; Groot, M. L. *Biophys. J.* **2008**, *94*, 4020−4030.
(46) Gross, R.; Wolf, M. M. N.; Schumann, C.; Friedman, N.; Sheves, M.; Li, L.; Engelhard, M.; Trentmann, O.; Neuhaus, H. E.; Diller, R. *J. Am. Chem. Soc.* **2009**, *131*, 14868−14878.
(47) Diller, R.; Jakober, R.; Schumann, C.; Peters, F.; Klare, J. P.; Engelhard, M. *Biopolymers* **2006**, *82*, 358−362.
(48) Herbst, J.; Heyne, K.; Diller, R. *Science* **2002**, *297*, 822−825.
(49) Haran, G.; Morlino, E. A.; Matthes, J.; Callender, R. H.; Hochstrasser, R. M. *J. Phys. Chem. A* **1998**, *103*, 2202−2207.
(50) Kandori, H.; Furutani, Y.; Nishimura, S.; Shichida, Y.; Chosrowjan, H.; Shibata, Y.; Mataga, N. *Chem. Phys. Lett.* **2001**, *334*, 271−276.
(51) Schoenlein, R. W.; Peteanu, L. A.; Mathies, R. A.; Shank, C. V. *Science* **1991**, *254*, 412−415.
(52) Smith, S. O. *Annu. Rev. Biophys.* **2010**, *39*, 309−328.